Geologia Croatica	68/3	247–259	11 Figs.	1 Tab.		Zagreb 2015

Structural controls on petroleum migration and entrapment within the faulted basement blocks of the Szeghalom Dome (Pannonian Basin, SE Hungary)

Molnár, László, M. Tóth, Tivadar and Schubert, Félix

Department of Mineralogy, Geochemistry and Petrology, University of Szeged, Egyetem u. 2., H-6722, Szeged, Hungary (molnar.laszlo@geo.u-szeged.hu)

doi: 10.4154/gc.2015.19

Geologia Croatica

ABSTRACT

The basement of the Pannonian Basin contains several fractured metamorphic hydrocarbon reservoirs that typically form structural highs between the Neogene sedimentary sub-basins. One of the largest reservoirs, the Szeghalom Dome, is located on the northern margin of the Békés Basin and is mainly composed of Variscan gneisses and amphibolites with different metamorphic evolutions. These petrologically incompatible blocks were juxtaposed by post-metamorphic tectonic activity that was accompanied by the formation of brittle fault zones with higher transmissibilities.

The aim of this study was to define the spatial arrangement of these fault zones and their internal architecture by integrated evaluations of borehole core and well-log data from a group of wells in the central part of the field. Spatial correlations between the reconstructed 1D lithologic columns revealed the main structural elements of the Szeghalom Dome. The low-angle (<15°) thrust faults most likely developed due to north-northwest vergent Cretaceous nappe tectonics, which were probably responsible for the juxtaposition of the different metamorphic blocks. A complex system of normal faults throughout the basement high provides evidence of intense Miocene extensional tectonic activity. This phase of the geodynamic evolution of the basin is believed to be responsible for the horst-graben structure of the Szeghalom Dome.

The integration of the structural results with datasets of the palaeo-fluid evolution, recent production and fracture network geometry, indicates the importance of these fault zones in both the migration of hydrocarbons from the adjacent sub-basins to the overlying sediments and the development of significant storage capacity within the strongly fractured rock masses, (mainly the amphibolite bodies). These observations of fluid flow also emphasized the impact of strong anisotropic permeability anisotropy of the faults throughout the fractured reservoir.

Keywords: Fractured reservoir, Variscan basement, Fault zones, Well-log interpretation, Fault rock analysis

1. INTRODUCTION

Brittle fault zones have a key role in the hydrodynamics of fractured reservoirs (NELSON, 2001). They can behave as barriers, conduits or as a combination of both (CAINE et al., 1996), so understanding their internal structure is crucial. Previous studies (CAINE et al., 1996; EVANS et al., 1997; MOLNÁR et al., 2014) on the make-up of fault zones defined two main structural elements: 1) the weakly disaggregated, densely fractured "damage zone", which is generally associated with higher conductivity and permeability relative to the undeformed protolith; and 2) the intensively de-

formed and fragmented fault core, where the pre-existing rock fabrics have been destroyed by the development of the fault and have been replaced by fault rocks.

Several studies have revealed that the formation of the fault core is often coupled with a significant decrease in permeability (EVANS et al., 1997; WIBBERLEY & SHIMAMOTO, 2003; STORTI et al., 2007), which is mainly a result of cataclasis, clay smearing or clay gouge formation and cementation (MOELLER-PEDERSEN & KOESTLER, 1997; MANZOCCHI et al., 2010). The geometry of the juxtaposed lithologies and their relative transmissibility are also important factors in the conduit/barrier behaviour of fault zones (ALLAN, 1989). The hydraulic character of the deformed zones is further complicated by their strong anisotropic permeability (EVANS et al., 1997). The highest permeability evolves parallel to the fault plane and the slip vector. In contrast, the hydraulic conductivity is one to four orders of magnitude lower parallel to the fault plane and perpendicular to the slip vector. Similar characteristics can be observed perpendicular to the fault plane and the slip vector. These can result in many types of hydraulic behaviour of faults depending on the widths of distinct structural elements (damage zone and the fault core) with respect to the total width of the fault zone: localized conduits, localized barriers, distributed conduits or combined conduits-barriers (CAINE et al., 1996).

The large-scale spatial interpretation of fault zones in hydrodynamic systems can be problematic, especially with a lack of borehole cores, packer measurements or sophisticated modeling because the main structural elements are often below the limit of seismic resolution (BEN-ZION & SAMMIS, 2003). This phenomenon increases the value of data available from cores and well-logs and suggests the importance of their integration and calibration.

This study focuses on the Pannonian Basin (PB), which is part of the Alpine-Carpathian-Dinaric orogenic belt. Due to its complex Mesozoic-Neogene evolution (e.g., TARI et al., 1992; CSONTOS & NAGYMAROSY, 1998), the southeastern part of the PB consists of deep sub-basins that are separated by metamorphic basement highs (e.g., TARI et al., 1999; M. TÓTH et al., 2009). In many cases, these blocks act as fractured water and hydrocarbon (HC) reservoirs in which the brittle fault zones play an important role in fluid storage and migration. One of the best known basement highs is the Szeghalom Dome (SzD), which is also one of the largest fractured basement HC reservoirs in the PB (NELSON, 2001). According to unpublished industrial reports however, only a small portion of the accumulated hydrocarbons has been produced because of the complex structural and lithological architecture of the SzD. Here, we attempt to reconstruct the structural evolution of the study area and determine the role of the internal architecture of the fault zones in the local fluid flow regimes. Moreover, correlation of the palaeo-fluid evolution with the recent hydraulic features of the SzD was another aim of this work. In the recent case, well-test results and earlier fluid inclusion data were available to estimate both the past and current hydraulic characteristics of the analyzed fault zones.

2. GEOLOGICAL SETTING

Due to its complex multistage tectonic history, the Pannonian Basin is a complicated mosaic of structural blocks with different patterns of geological evolution. The crystalline basement of the PB is mainly composed of Variscan metamorphic rocks with significantly different pressure-temperature-time histories (SZEDERKÉNYI et al., 1991). The SzD is one of the best known units and has a heterogeneous lithological composition (M. TÓTH, 2008; Fig. 1).

The northern part of the SzD and the neighbouring areas are mainly composed of orthogneiss that is derived from the medium-grade metamorphism of an igneous intrusion. In some borehole cores, undeformed microgranite dykes have no textural indications of metamorphism. These lithologies are jointly called the OG group. In the central and southern parts of the SzD, two other types of gneiss are dominant. The SG group is composed of high metamorphic grade sillimanite and garnet-bearing biotite gneiss that is often coupled with garnet-bearing amphibolite. In contrast, amphibolite and amphibole-biotite gneiss (AG group) with medium grade metamorphism is common at the uppermost structural level. These metamorphic blocks with distinct evolutions (M. TÓTH, 2008) were juxtaposed as a result of post-Variscan structural movement.

The most significant tectonic event after the Variscan metamorphism was the Eoalpine compressional tectonic phase (Austrian, Laramian time sequences), which formed complicated nappe systems throughout the basement of the Pannonian Basin. Several studies have demonstrated the existence of nappe tectonics in the PB (POSGAY et al., 1995; TARI et al., 1999), which resulted in the widespread formation of subhorizontal, north-northwest-directed thrusts throughout the basement. Later back-arc type extension during the middle Miocene resulted in the formation of metamorphic core complexes coinciding with the exhumation of a series of crystalline domes along low-angle normal faults (HORVÁTH et al., 2006). These structures were further complicated by sinistral strike-slip fault zones with significant horizontal displacements (ALBU & PÁPA, 1992). During the Badenian, the intense extension formed horst-graben structures along north-south striking normal faults (M. TÓTH, 2008).

As a result of the complex post-metamorphic evolution of the SzD, a dense fracture network with significant fluid storage capacity developed (M. TÓTH, 2008). Previous analyses of the fracture network (M. TÓTH et al., 2004) and fracture-filling mineral assemblages (JUHÁSZ et al., 2002) demonstrated the significant difference in rheological behaviours of the amphibolite and gneiss bodies. This difference led to the development of a fracture network that is above the percolation threshold of the amphibolites; in contrast, the fracture network in the gneisses is usually below this limit and contains unconnected fracture systems (M. TÓTH et al., 2004). The higher storage capacity of amphibolites compared to the gneisses is also demonstrated by palaeo-fluid reconstructions of the SzD (SCHUBERT, 2003; SCHUBERT et al., 2007), which reported hydrocarbon-bearing fluid inclu-

sions exclusively from the amphibolite bodies and the damage zone of the faults.

The wide fault zones that separate blocks of different metamorphic evolution patterns within the SzD may have a key role in the communication between the crystalline basement and the neighboring sedimentary basins; because the flanks of the SzD are surrounded by relatively deep sedimentary sub-basins with significant overpressures, the fractured basement can act as a migration pathway from the juxtaposed sediments to the overlying sediments (VASS et al., 2009). These brittle fault structures can also link separated amphibolite bodies (M. TÓTH, 2008; VASS et al., 2009).

Based on sedimentological and organic-geochemical evidence, the main sources of the hydrocarbons that are currently produced from the Szeghalom Dome basement reservoir are believed to be the middle to upper Miocene shales (TELEKI et al., 1994). Following the Badenian exhumation, the SzD formed an island in the Late Miocene Pannonian Lake. The basal conglomerate (Békés Formation) covered the coastal zones of the basement, while the local basinal clay marl aquitard (Endrőd Formation) either overlaid the conglomerate or rested directly on the metamorphic domes. This marl grades upwards into a thick succession of turbidite-rich (Szolnok Formation) and slope (Algyő Formation) sediments, which are thinner but coarser grained above the basement highs (MÁTYÁS, 1994) and represent a possible pathway for vertical migration (JUHÁSZ et al., 2002). During the "post-rift" phase of the basin evolution, the exposed metamorphic highs subsided ("thermal subsidence"; HORVÁTH et al., 1988; M. TÓTH, 2008) to a depth of approximately 3 kilometres and provided pathways for fluid migration and/or storage (JUHÁSZ et al., 2002). According to TELEKI et al., 1994, the recently produced hydrocarbons of the SzD most likely generated in the adjacent overpressured sub-basins located south of the SzD, such as the Békés Basin and the Vésztő Graben (Fig. 1).

3. SAMPLES

The study area is located north of the highest part of the SzD (Fig.1/c), where the top of the basement is composed of rocks of the AG group. SG group rocks are located in the deeper parts of the basement and are separated from the AG group rocks by wide brittle fault zones.

The borehole cores used for the petrographic analysis are from wells A-11, -20, -22, -180: the depth intervals of the samples are summarized in Table 1. The most important well (A-180) is located north of the central, highest part of the SzD and intersects a major fault zone. Core recovery from the fault zone is nearly 100%. The fault zone separates the lithologic units of the AG group in the hanging wall and the SG group in the footwall. The examined section is approximately 20 metres wide and extends from a depth of 1913 metres to 1936 metres; it is primarily composed of brit-

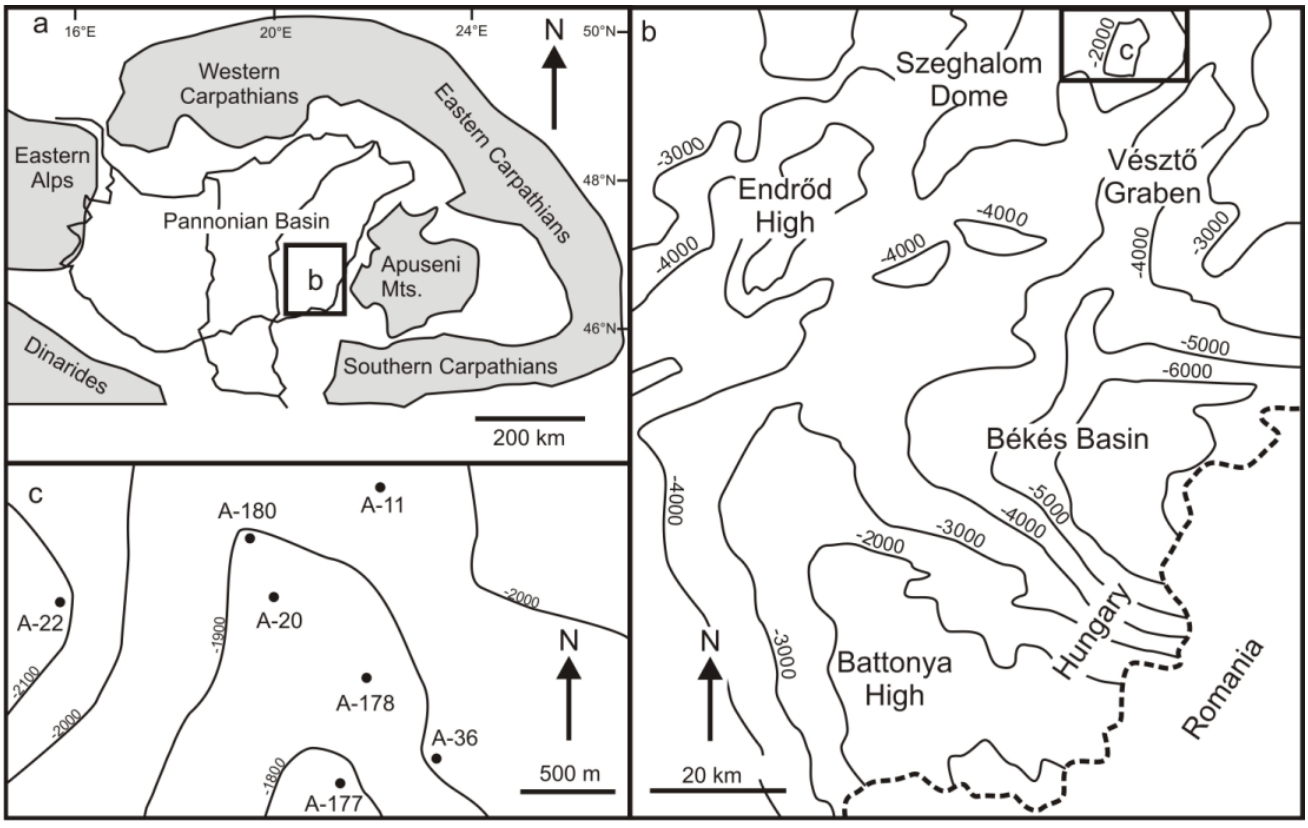

Figure 1: a) Location of the Szeghalom Dome in the Pannonian Basin and its geological environment. **b)** Szeghalom Dome in the eastern part of the Pannonian Basin with the adjacent sub-basins and elevated basement highs. **c)** Locations of the sampled wells in the central part of the SzD. The contour map indicates the depth to the basement in metres.

Table 1: The available borehole cores with their intervals, in metres below sea level.

Well number	Depth intervals of the borecores (meters below sea level)
A-11	1957–1968
	2007–2009
A-20	1901–1903
	1976–1979
A-22	2117–2119
A-180	1913–1936

tle fault rocks with different degrees of deformation (Fig. 2). The cores were not oriented, so their proper structural interpretation was not available. Nevertheless, the thin sections were made parallel with the lineations and perpendicular to the foliations, where it was possible. Samples of both the undeformed footwall and the hanging wall were analyzed to define their well-log properties.

Well-log analysis was applied to the wells A-11, -20, -22, -36, -177, -178 and -180. The well-log data were provided by the MOL Hungarian Oil and Gas Company. The well-log measurements were recorded every 20 cm for the following parameters: spontaneous potential (SP), caliper width (Cal), resistivity (Res), density (Den), compensated neutron porosity (CN), acoustic velocity (AC) and natural gamma logs (GR).

4. METHODS

The available borehole cores were analyzed petrographically at both meso- and micro-scales. The tectonites were classified according to their clast geometric parameters as described in MOLNÁR et al. (2014).

The well-log data were calibrated on the depth intervals that overlapped with the petrographically analyzed cores. The data set was statistically evaluated using the IBM SPSS 20.0 statistics software. The discriminant function analysis method was used to separate the lithologic groups based on their well-log properties (the forward stepwise method using Wilks' lambda) (Fig. 3/a). First, a discriminant function was computed to define the difference between the undeformed wall rock (AG and SG together) and the tectonized depth intervals by calculating the proper linear combination of the measured well-log data (Fig. 3/b). Discriminant functions were then calculated to define the different types of fault rocks (fault breccia, cataclasite, fault gouge) within the zones that were classified as tectonized in the previous step (Fig. 3/b). Both types of discriminant functions were cross-validated to test the efficiency of the prediction model. The computed functions were then applied to the depth intervals of the analyzed wells where the lithology was unknown.

5. RESULTS

5.1. Petrography

The internal structure of the shear zone in well A-180 reflects the diversity of the petrographic characteristics of the different types of tectonites (fault breccias, cataclasites and fault gouges) (Fig. 2). Samples from A-11, A-20 and A-22 composed of strongly fractured and partly brecciated gneisses from the AG lithologic group. Intact borehole core from the SG group was available only from one well (A-11: 2007-2009 m) with sillimanite-bearing biotite gneissic composition.

Most of the analyzed samples in A-180 were composed of coarse fault breccia that contained weakly disaggregated structures and clast sizes that were typically greater than the cm-scale (Fig. 2/a-b). The particles in these samples are only weakly rotated and often fit together along their sharp, angular dilatational edges, reflecting a typical jigsaw puzzle texture (MORT & WOODCOCK, 2006). These weakly disaggregated fault breccia particles usually have a chaotic structure and lack a clast shape preferred orientation. The particles are dominantly composed of rock fragments that are derived from the wall rock and have a recognizable gneiss precursor, while single mineral fragments are subordinate in the fault breccias. A few samples of the breccias have similar internal structures; those with smaller clasts are regarded as micro-breccias, and the coarse fault breccias are often embedded in greenish chlorite or brownish iron-oxide (hematite) cement. Precipitation of Fe phases is always visible on the margins of the angular clasts.

Several samples show characteristic features of cataclastic deformation that resulted in a decrease in clast size and an increase in the matrix ratio, while the preferred local orientation of the clasts is defined by their long axes (Fig. 2/c-d). The fractured grains are often accompanied by deformed phyllosilicate flakes, which implies locally brittle-ductile transitional deformation. The fragmentation in the cataclasite samples makes the protolith of the crushed particles difficult to define because they are often monomineralic (composed mainly of quartz or feldspar). Iron-oxide cement is also often present, in contrast to the missing chlorite cement.

A third type of samples, the incohesive fault gouges, is present in thin deformational bands (Fig. 2/e-f). These bands are mainly composed of strongly comminuted mono-crystalline (mainly quartz) particles; only a few survivor rock fragments are observable. The isolated fragments are surrounded by the completely crushed parts of the protolith and the fabric of these samples also indicates a semi-brittle style deformation. These fault gouge zones are usually a few cm wide and presumably define the localized slip zones of the faults, which are probably the locations of the most intensive displacements. The kinematics of the observed slip surfaces and their structural interpretation were not possible to determine in the lack of oriented cores. Nevertheless, in the micro-scale evaluations the reverse micro-faults and the manners of the compressional activity were predominant.

The fault zone in well A-180 is mainly composed of weakly disaggregated, coarse fault breccias: the detailed lithologic composition of the interval is visible in Figure 3/a. Despite their fragmented texture, the fault breccia core samples reflect a hardened and mechanically intact structure (Fig. 4/a-b). The cohesiveness of the samples was most likely retained due to the pervasive multistage cementation along the

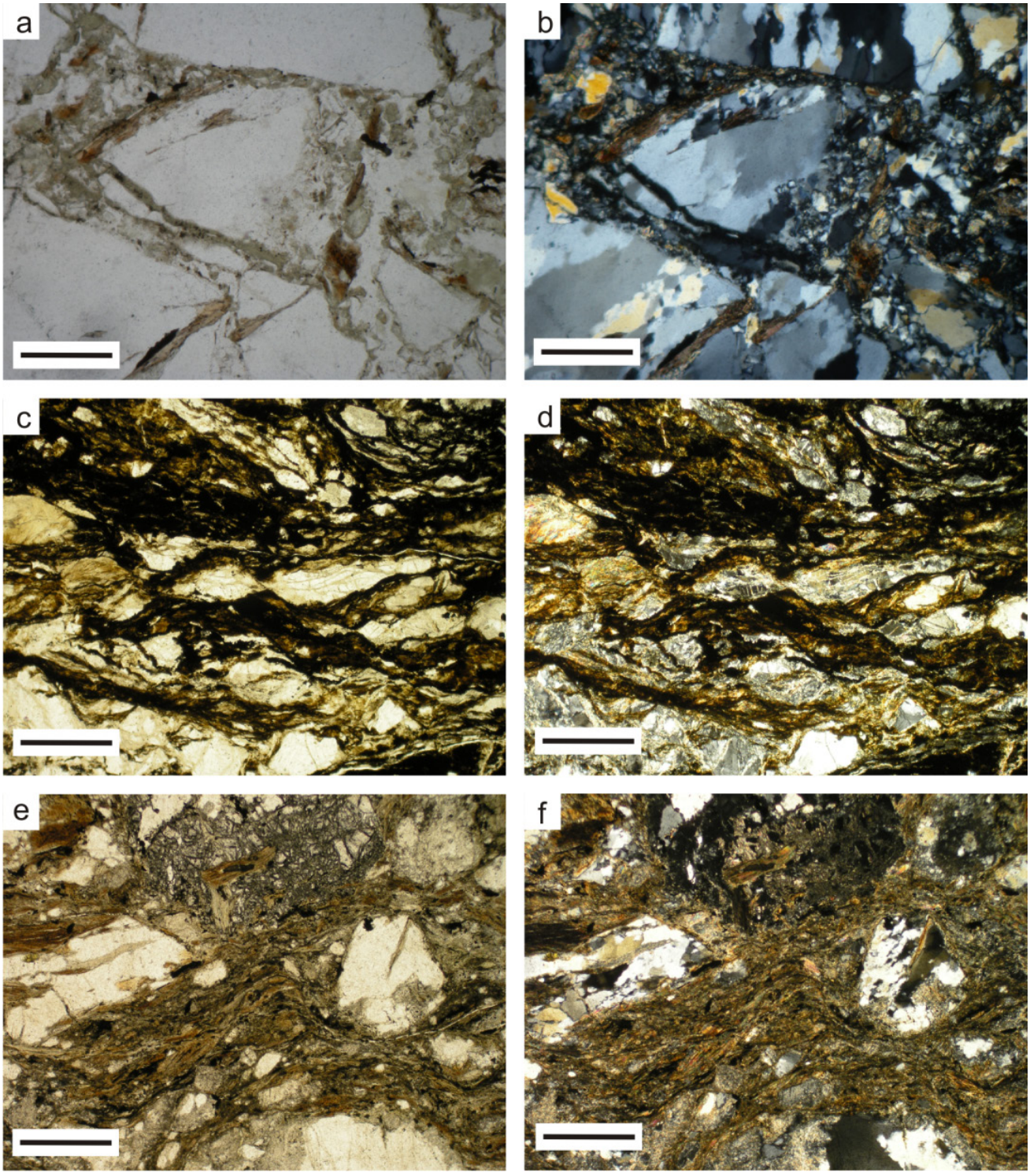

Figure 2: Thin sections in the fault zones. **a, b)** Coarse fault breccia with gneissic rock fragments (1N, +N) (well A-180). **c, d)** Oriented, elongated clasts in cataclastic fabric (1N, +N) (well A-180). **e, f)** Layers of comminuted gouge containing primarily crushed mono-crystals (1N, +N) (well A-180). The scale bars are 500 μm long.

fault zone, which was also described by earlier works (JUHÁSZ et al., 2002, SCHUBERT et al., 2007): these cement minerals are mainly chlorite, calcite, hematite and partly quartz. Although the fault breccias have a hardened structure, often cm-scale open pore space could be preserved in these cores, which likely maintain the higher permeability of the samples. This intensely fractured host rock presumably forms the damage zone of the fault zone. In contrast, the zones of cataclasite and fault gouge are up to one meter wide and are considered as the fault cores; they are most clear at three distinct depth intervals (1917, 1922 and 1926 metres below sea level) (Fig. 3/a). These samples dominantly have an incohesive structure: cores can be broken into components with fingers (Fig. 4/c-d) and a weak drop was also observed

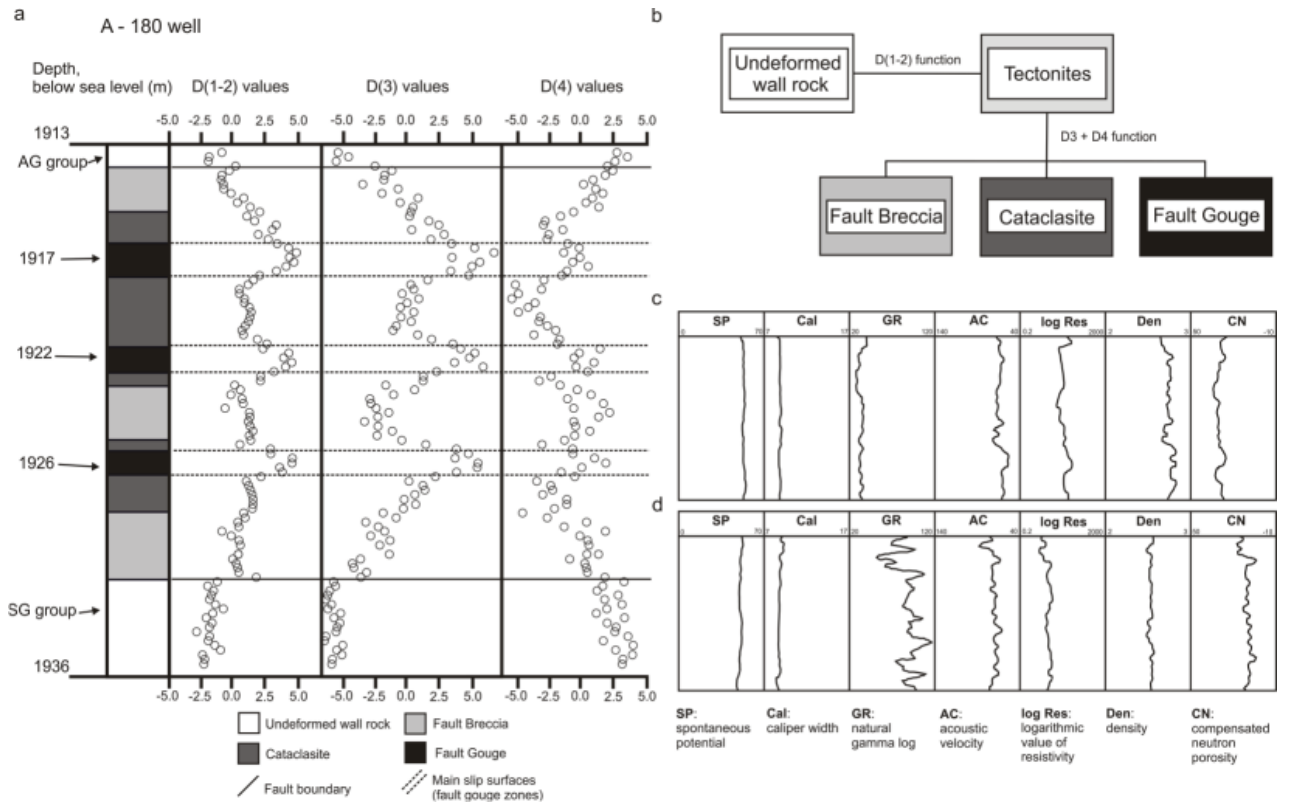

Figure 3: Details of the log-to-core calibration. **a)** Lithological composition of the fault zone in well A-180 with the calculated D(1-2),(3) and (4) values. The fault gouge-bearing intervals at 1917, 1922 and 1926 metres indicate the locations of the largest displacements. **b)** Theoretical workflow for the determination of the lithologic architecture in the analyzed wells. Functions D(3) and D(4) are applied only when D(1-2) defines the sample as a tectonite. **c,d)** Representative well-log sections for undeformed (C) and deformed (D) depth intervals, which are verified with core data.

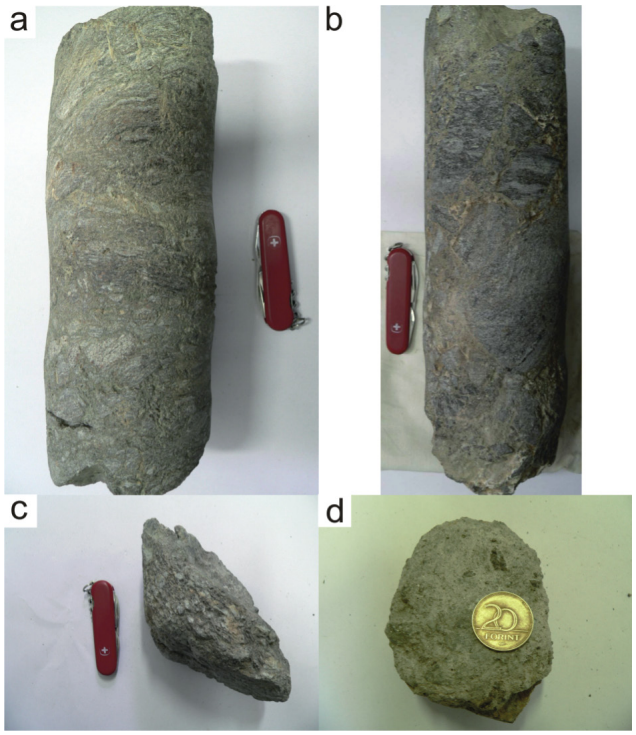

Figure 4: Characteristic core samples from the fault zone of A-180. **a,b)** Cohesive, coarse grained fault breccia core. The structure of the sample is intact, despite the pervasive brittle deformation and fragmentation. **c,d)** Incohesive fault rock samples from the presumed fault core of the shear zone. The most intense deformation is accompanied with the mechanical weakening of the tectonites.

in the core recovery ratio of these intervals (by unpublished industrial reports). Increasing deformation is thus usually coupled with the significant weakening of the fault core. The cataclasite and fault gouge surfaces are structurally confined between horizons of coarse fault breccia. As in previous studies (e.g., EVANS et al., 1997), the fault cores are typically one meter thick; the fault cores imply the localization of strain within the fault zone and mark the locations of largest displacement.

5.2. Well-log data

To extend the lithologic data from the cores to the other intervals of wells, calibration with well-log data was necessary. The proper combination of well-log data was calculated by applying discriminant functions analysis to separate the distinct lithologies (Fig.3/b).

The undeformed host rock (Fig. 3/c) and the tectonized samples (Fig. 3/d) were separated using the following discriminant function:

$$D(1\text{-}2) = 1.1 * \text{natural gamma (GR)} - 0.5 * \text{resistivity (Res)} - 0.9 * \text{density (Den)}$$

The calculated function successfully discriminated the undeformed host rock and the tectonized intervals without any overlap (Fig 5/a). To define the internal structure of the tectonized zones, the lithologically-known fault rocks (fault

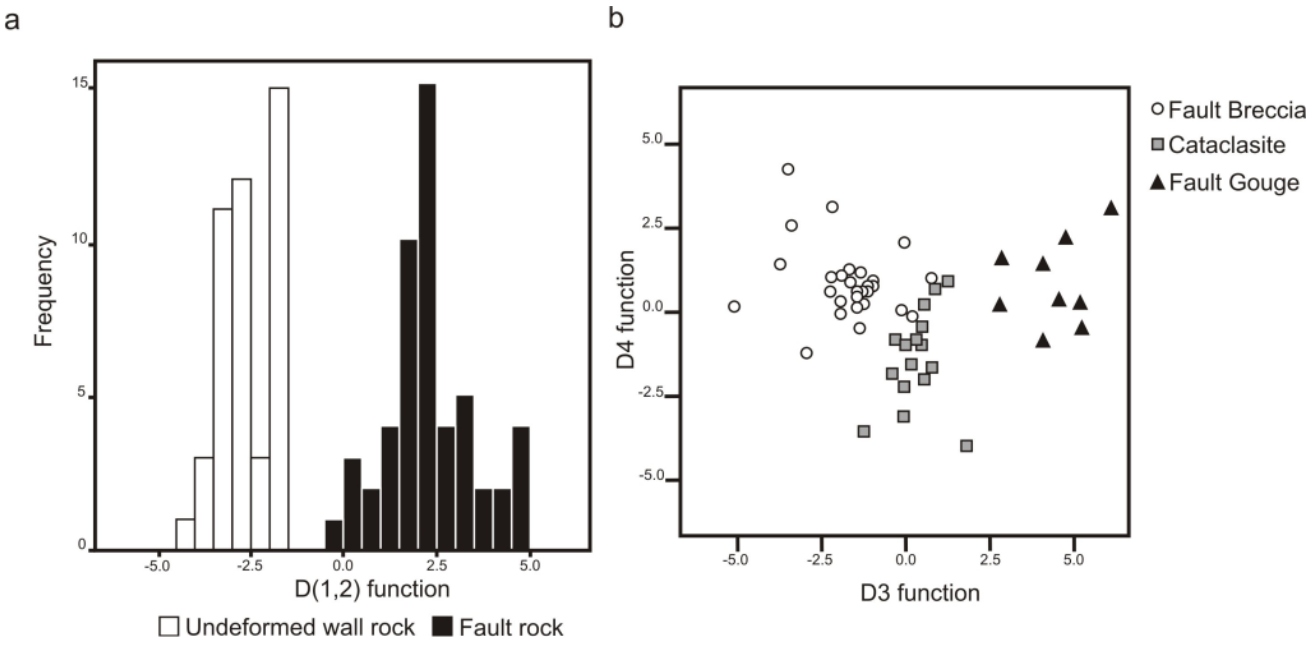

Figure 5: a) Separation of the deformed and undeformed depth intervals using the scores of the calculated D(1-2) function. The most important well-log parameters used to discriminate the intervals were the natural gamma, density and resistivity values. **b)** Discrimination of different fault rock types with the calculated D3 – D4 functions, which are mainly based on the compensated neutron porosity, resistivity, density and natural gamma log values.

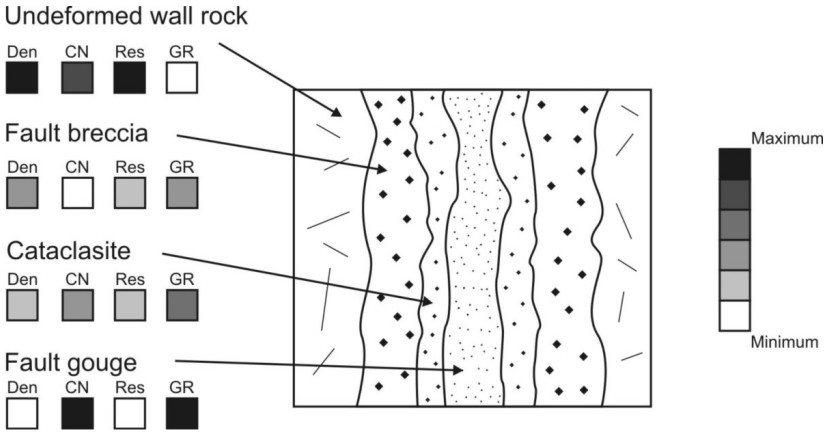

Figure 6: Spatial variations of the most important well-log parameters for an idealized fault zone. The darker colours indicate greater parameter values. According to this interpretation, the deformation is often associated with decreasing density and resistivity towards the core zone. The most significant porosity enhancement develops in the weaker fragmented and brecciated zones. Res: resistivity, Den: density, CN: compensated neutron porosity GR: natural gamma.

breccia, cataclasite and fault gouge) were then separated using two discriminant functions:

$$D3 = 0.7 * \text{compensated neutron porosity (CN)} - 0.5 * \text{resistivity (Res)}$$

$$D4 = 0.6 * \text{density (Den)} - 0.9 * \text{natural gamma (GR)}$$

These two discriminant functions clearly separated the different fault rocks, especially the clay-rich fault gouge samples (Fig. 5/b). These functions were then applied to classify the lithologically-unknown depth intervals of wells A-11, -20, -22, -36, -177, -178 and -180 to determine their lithologic and structural compositions.

6. SPATIAL EXTENSION OF PETROLOGICAL AND WELL-LOG DATA

6.1. Well-log properties of the lithologies

The weights of the parameters in discriminant function D(1-2) define the main geophysical differences between the undeformed protolith and the tectonized zones (Fig. 5/a). The greatest factor in the difference is the high natural gamma ray values, which implies a raised amount of clay minerals that is presumably caused by the intensely weathered and altered host rock in the fault zone (Fig. 6). The relatively lower electrical resistivity of the tectonites reflects their strongly fractured/fragmented characteristics, which results

in stronger fluid infiltration into these zones. The lower densities are probably related to the presence of the higher fracture density in the tectonized zones, which is often coupled with porosity enhancement (Fig. 6).

The petrographic and well-log properties of the diverse tectonite types are distinctly different (Fig. 5/b), which reflect the internal structure of the fault zones. According to function D3, higher levels of deformation are manifested in increases of the compensated neutron porosity values and further decreases of the electric resistivity. In function D4, higher density and lower gamma-ray values are characteristic. These suggest that the intensely deformed parts of the fault zones (cataclasites and fault gouges) can be characterized by low densities and resistivities and that further elevated natural gamma activity and compensated neutron porosity values mark the fault core, which is consistent with the observations of HUNG et al. (2007) and JEPPSON et al. (2010). The density and resistivity logs imply intensive fracturing, fragmentation and comminution, while the natural gamma and neutron porosity values indicate strong weathering and clay mineral formation with significant porosity reduction (Fig. 6). In contrast, the interpreted damage zone with coarse fault breccias has higher density and resistivity values and lower gamma and neutron porosity values (Fig. 6). These suggest that the weaker disaggregated zones can maintain a significantly higher porosity than the comminuted fault core.

6.2. Structural interpretation of the analyzed part of the SzD

The application of the discriminant functions described above to the well-log data from wells A-11, -20, -22, -36, -177, -178, and -180 provided an opportunity to determine the lithologies that were present in these wells and to understand the structural evolution of the SzD (Fig. 7). Based on the available data, three groups of wells can be distinguished from the seven wells: two triplets (A-180, -11, -20 and A-36, -177, -178) and a block containing one well (A-22).

The most important well was A-180 because the large number of core samples provided useful information about the architecture of the SzD. The fault zone in well A-180 contains strong structural heterogeneities between the depths of ~1915 and 1935 metres, where the three main cataclasite and fault gouge-bearing zones are always embedded in coarse fault breccia members (Fig 3/a). These comminuted planes – especially the clay-rich gouge zones – can act as the slip zones of the fault zones, and their presence indicates strain localization. An interpretation of the well-log from well A-20, (which is the closest well to A-180), indicates that it also contains a distributed fault zone with wide, gouge-bearing fault core between ~1990 and 2005 metres (Fig. 7). Although no core was collected across this interval, the well-log data indicate that the two wide tectonized intervals in the

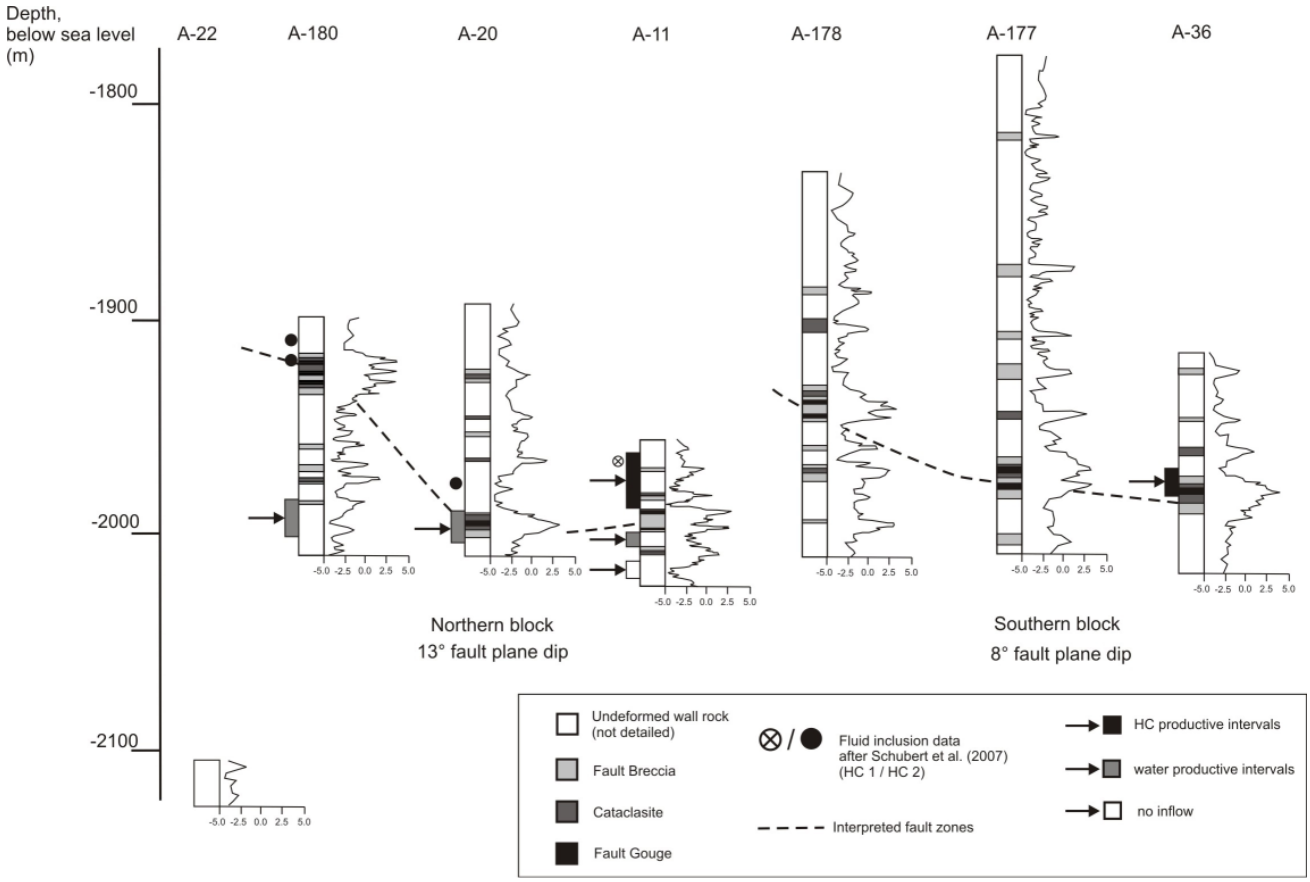

Figure 7: The interpreted lithological compositions of the analyzed wells. The dashed line indicates the observed low-angle fault surfaces. The wells form two triplets, including a northern and a southern block. Along with the lithological composition, the calculated D(1-2) values are also illustrated along the 1D section of the wells.

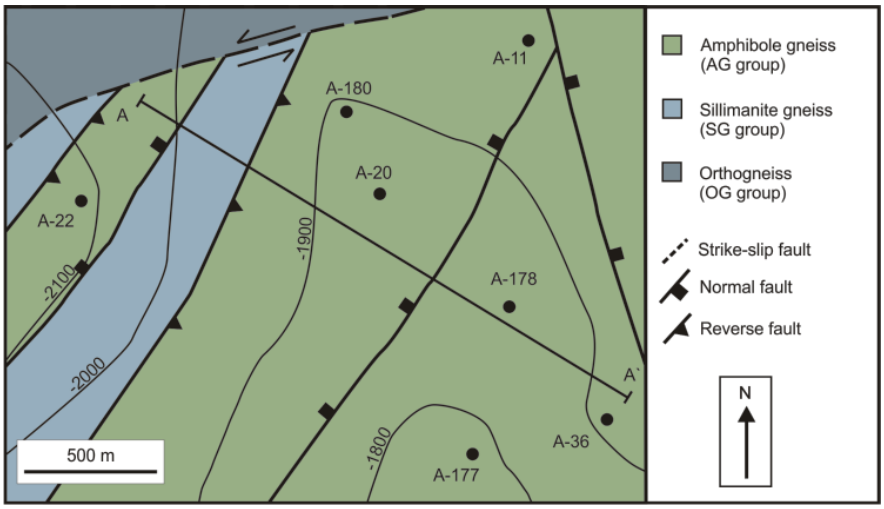

Figure 8: Basement map of the Szeghalom High with the major interpreted structural elements. The contour map indicates depth to the basement in metres. The Cretaceous nappe structures were overprinted by complex Neogene normal faulting. Note that members of the AG group dominate at the top of the basement. For details of transect A-A', see Figure 9.

neighbouring wells are parts of the same fault zone. Similar gouge-bearing, distributed fault zones with wide damage zones are present in well A-11 at approximately the same depth interval (≈1985–2000 m) as in A-20 (Fig. 7). These three occurrences of the interpreted shear zone define a low angle (13°) fault plane that dips to the southeast. Other more weakly fragmented and thinner fault planes are also observed in these wells but do not contain cataclasite gouge-bearing (slip) zones. These data suggest that the fault cores were the locations of the largest displacements and can be considered a major fault zone (Fig. 7).

Wide tectonized zones that indicate relatively large displacements are present in well A-178 at depths of ≈1925-1945 metres. Similar zones are also present at similar depths in wells A-177 and A-36; however, the interval is slightly thinner in A-36 (A-177: ≈1955-1970 m, A-36: ≈1960-1980) (Fig. 7). These depth intervals also include the gouge-bearing slip zones, which imply that these intervals have a similar origin to the shear zone in wells A-11, -20, and -180. In this sense, the fault zone in the southern group of wells (A-36, -177, and -178) is the continuation of the zone found in the northern group with a slightly smaller dip angle (8°) but a similar south-southeast dip. Although the small amount of available information only allows a rough estimate of the geometry of the fault planes, and there is a slight difference in the dip angles and directions, the faults in these groups of wells were likely affected by a similar deformational event.

Based on the interpretation of several analogous examples from the crystalline basement (e.g., PAP, 1990; TARI et al., 1999), these fault zones can be interpreted as a low-angle thrust with a northwest vergence. This explanation is consistent with the reinterpretation of 2D seismic profiles from the metamorphic basement (M. TÓTH et al., 2009). Because these old seismic surveys mainly focused on the overlying clastic sediments, they provided only sporadic reflectors from the crystalline basement. Using sophisticated seismic interpretation techniques, M. TÓTH et al. (2009) defined the largest structural elements and characterized most of them as low-angle thrust surfaces.

Earlier studies reported that the formation of these low angle (≈5-15°), northwest-vergent thrust sequences throughout the basement of the Pannonian Basin are related to Eoalpine compressional activity during the Late Cretaceous nappe formation (TELEKI et al., 1994; TARI et al., 1999, KOVÁCS et al., 2000). The AG and SG lithologic groups, with their distinct metamorphic pathways, were juxtaposed by this Eoalpine nappe activity. This event is presumably also responsible for the formation of fault zones on the SG-OG contact, according to the results of unpublished industrial reports.

The repeated presence of the thrust surfaces and their spatial arrangement indicate post-Cretaceous tectonic activity between the northern and the southern groups of wells, which cross-cut the initially approximately uniform thrust surface (Figs. 7 and 8). The dip of the thrust and the depth of the tectonized intervals indicate high angle extension with approximately 150 metres of vertical displacement combined with tilting of the northern hanging wall block (Fig. 9). A similar tectonic style is indicated in well A-22, which reached the basement surface approximately 200 metres deeper than in the adjacent wells and penetrated only ~20 metres of basement rocks of the AG group (Fig. 7). Because the AG group is in the highest structural locations in the SzD (M. TÓTH, 2008) (Fig. 8) and always forms the top of the basement, the significant vertical difference between wells A-22 and A-180 is probably also the result of post-Cretaceous motion (Fig. 9).

Extensional tectonic activity has been widely reported in the SzD and can be related to the formation of horst/graben structures during the syn-rift stage of the opening of the Pannonian Basin during the Miocene (M. TÓTH, 2008). As a result of the complex evolution of the PB, this type of structure is most common in the central part of the basin; in contrast, the degree of extension at the basin margins was high enough to form metamorphic core complexes (HORVÁTH et al., 2006). This phase of basin evolution culminated in the uplift and the exhumation of the SzD from a relatively shallow depth (<10 km) and the subsidence of nearby sub-basins (e.g., Békés Basin) (TELEKI et al., 1994; M. TÓTH, 2008).

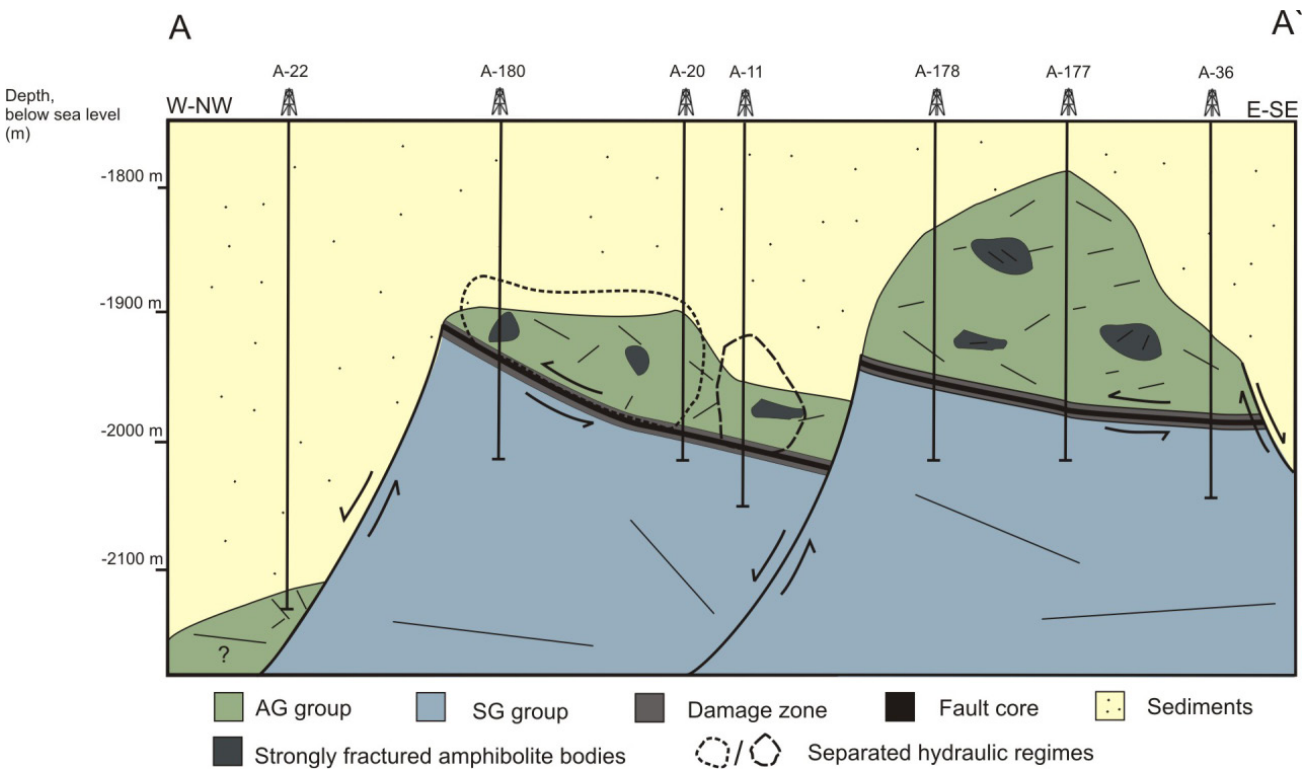

Figure 9: West-northwest – east-southeast cross section of the Szeghalom Dome. The dashed lines indicate the separate palaeo-fluid systems based on previous fluid inclusion results (SCHUBERT et al., 2007). The Late Cretaceous nappe surfaces were cut by high angle Neogene normal faults. Significant storage capacity in the basement is exclusively related to amphibolite bodies in the AG group. The composition of the basement is unknown below well A-22. The horizontal components of the cross section are not to scale.

6.3. Discussion of palaeo-fluid regimes in the analyzed part of the SzD

In this section, the new structural data are integrated with the results of previous studies, particularly with respect to the hydrodynamic characteristics of the SzD (Fig. 9). M. TÓTH et al. (2004) found that the densely fractured amphibolite bodies in the AG group contain significant storage capacity in the metamorphic blocks of the SzD.

The previously reconstructed palaeo-fluid evolution was based on analyses of aqueous and petroleum inclusions in the fracture-filling quartz crystals, primarily from the amphibolites and subordinately from the damage zones of faults (SCHUBERT, 2003; SCHUBERT et al., 2007). The fact that most of the analyzed fluid inclusions are present in the amphibolite zones, while they are totally absent from the gneisses, strengthens the interpretation that the main storage capacity is related to the intensely fractured amphibolite bodies. In this model, the damage zones of brittle faults served as migration pathways towards the amphibolites, the higher porosity of which was deduced from petrographic observations (coarse angular clasts with preserved pore space; c.f. Fig. 2).

The geochemical features and the degree of maturation indicate that the petroleum fluids from wells A-180 and A-20 have similar characteristics, in contrast to well A-11, which contains significantly different (less mature and/or more intensely degraded) hydrocarbon fluids trapped in petroleum inclusions. No fluid inclusion data are available from wells A-22, -36, -177, and -178. The fluid inclusion data suggest that the rocks encountered in wells A-20 and A-180 form a connected palaeo-hydrodynamic regime, while the rocks in well A-11 represent a separate fluid system, at least during the cementation of quartz in the fractures (Fig. 9). These data clearly indicate that even though these three wells are close to each other and are aligned along the same wide brittle shear zone (see Fig. 9), the rocks represent separate hydrodynamic regimes.

Several scenarios can explain the hydraulic compartmentalization of the SzD. An unlikely but possible scenario is related to the significant temporal/spatial variability in the density and porosity/permeability of the fracture network, which is probably caused by the multistage cementation and reopening of fractures (JUHÁSZ et al., 2002). In this scenario, the petroleum inclusions represent the stage of the evolution of the fracture network that was locally favourable for fluid inflow (after fracture opening/reopening), which was followed by cementation, fracture sealing and fluid inclusion entrapment. However, the spatial distribution of the open fractures at a particular time – and thus the favourable conditions for fluid inflow – was heterogeneous across the fracture network. This probably resulted in the local absence of entrapped hydrocarbon inclusions at a certain degree of maturity during the process of migration within the basement. As a result, this model implies the formation of temporarily separated hydraulic regimes, which provides a possible mechanism for the isolated fluid systems of the SzD. However, the absence of pervasive fracture propagation in diverse stress fields does not favour this theory.

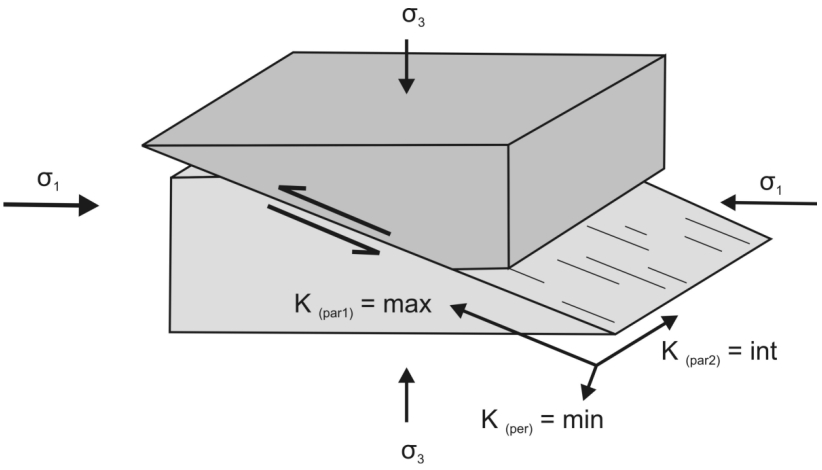

Figure 10: The permeability architecture of a thrust fault zone according to EVANS et al. (1997). The highest permeability values occur parallel to the fault plane and parallel to the slip direction ($K_{(par1)}$), and the lowest permeability values occur perpendicular to both the fault plane and the slip direction ($K_{(per)}$). Transitional permeability values occur parallel to the fault plane and perpendicular to the slip direction ($K_{(par2)}$). These results indicate that the fault zone has a significant (10^4) anisotropic permeability ratio.

The most likely scenario is compartmentalization due to the strong permeability anisotropy of the fault zones, which has been discussed by numerous authors (EVANS et al., 1997; ZHANG et al., 2001). Permeability anisotropy can be controlled by the shear displacement, effective stress, clay-smearing along the fault plane or anisotropic microstructure (GÉRAUD et al., 2006). These papers revealed distinct differences in permeability with anisotropy ratios as high as 10^4 (EVANS et al., 1997). The highest values are parallel to the fault plane and to the slip direction ($K_{(par1)}$) (Fig. 10). The lowest permeability values are perpendicular to both the fault plane and the slip direction ($K_{(per)}$), while transitional values were reported parallel to the fault plane and perpendicular to the slip direction ($K_{(par2)}$). This strong anisotropy can lead to hydraulic separation along the strike of the major fault zone in the SzD, as is observed in the different palaeo-fluid characteristics in the neighboring A-11 and A-20 wells. Moreover, the maximum permeability along the dip of the fault zone can explain the connected palaeohydraulic system encountered in wells A-20 and A-180 (Fig. 9).

The palaeo-fluid regimes within the SzD could also have been fragmented due to the intense multistage tectonic activity in the Neogene (LŐRINCZ, 1996). The interpreted structural architecture of the SzD supports this hypothesis. The normal faults probably disturbed the hydrocarbon migration in their vicinity (e.g., A-11, Fig. 7) and could have played a key role in the entrapment of the fluid inclusions with diverse chemical features (A-11 vs. A-20 and -180). It is difficult to determine whether these normal faults behaved as sealing faults or provided conduits for hydrocarbon migration towards the overlying clastic sediments. Nevertheless, the second hypothesis is supported by the results of JUHÁSZ et al. (2002) on the hydraulic connection between the basement and the overlying sediments.

It is unclear if the palaeo-fluid regime can be correlated with the recent hydrodynamic regimes. According to SCHUBERT (2003) and SCHUBERT et al. (2007), the palaeo-fluid migration recorded by the HC-bearing fluid inclusions occurred between the Cretaceous and the middle Miocene (Badenian). The onset of migration into the basement has been determined by biological marker compounds in the analyzed HC, the source of which could not have been generated before the Cretaceous (SCHUBERT, 2003). The data of JUHÁSZ et al. (2002) and SCHUBERT et al. (2007) indicate that the palaeo-fluid migration ended before the Badenian exhumation of the SzD. In contrast, based on industry data (TELEKI et al., 1994), the currently produced hydrocarbons of the SzD must be originated from the adjacent, deep sub-basins, such as the Békés Basin or the Vésztő Graben. Their source rocks were organic-rich shales with middle to upper Miocene ages and must be generated following the subsidence of the sub-basins (Fig. 11). These data suggest some dissimilarity between the palaeo- and the recent petroleum systems based on the possible source rocks.

Nevertheless, the results of the well-test data indicate several similarities between the palaeo- and recent fluid systems. In wells A-11 and A-36, the brecciated and intensely fractured damage zones of the thrust faults and the fracture system of the AG group have produced a significant amount of hydrocarbons (Fig. 7). Deeper water-producing intervals in A-180, A-20 and A-11 are also related to these permeable units but are below the oil-water contact. However, a well-test of well A-11 from the SG group did not show any inflow of fluid, indicating the impermeable nature of this lithological unit. This implies that the same structural elements participated both in the past and current migration and entrapment processes. Because of the limited width and spatial distribution of the low-angle thrust faults, these zones of elevated transmissibility can only act as migration pathways within the reservoir. In contrast, the extensive amphibolite blocks of the AG group in the hanging wall presumably form the main reservoir rock of the basement petroleum system.

According to the model for the mechanism of the recent flow systems of VASS et al. (2009), the SzD has a very strong hydraulic connection with the overlying and juxtaposed sediments because the elevated blocks of metamorphic basement can drain the adjacent overpressured basins below the local aquitard (Endrőd Formation) and have an important role in the compensation of their pressure conditions (Fig. 11). Due to its dense fracture network and numerous wide fault zones, the SzD behaves as a migration pathway towards the overlying clastic sediments (Szolnok and Algyő Formations); the relatively thin but rapid and notable fluid flux may have resulted in a so-called "chimney effect" in the internal parts of

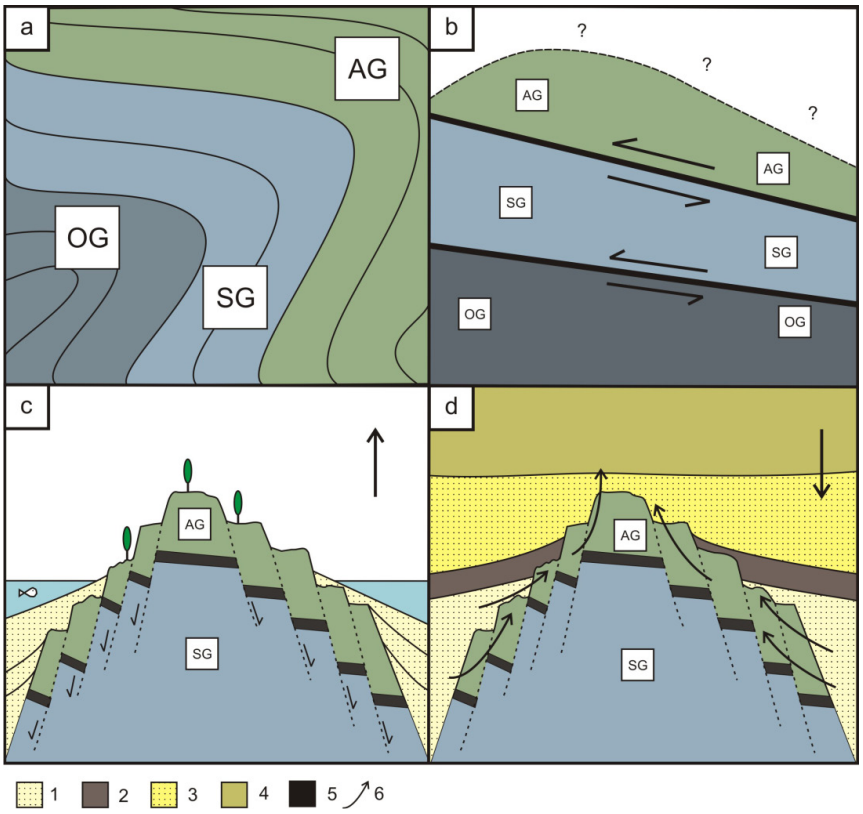

Figure 11: Schematic model of the geodynamic and hydrodynamic evolution of the Szeghalom Dome. **1:** Coastal conglomerate (Békés Formation), **2:** Basal clay marl, which forms a local aquitard (Endrőd Formation), **3:** Turbidite-rich sediments (Szolnok Formation), **4:** Delta slope sediments (Algyő Formation), **5:** Main brittle fault zones, **6:** Regional fluid flow system. **a)** Simplified cross section of the Variscan multistage metamorphism of the lithological groups at diverse pressure and temperature conditions. **b)** Late Cretaceous nappe tectonics along low-angle thrust faults, which juxtaposed the AG, SG and OG lithological groups. Deformation took place at shallow depths and with unknown overlying rocks. **c)** Middle Miocene (Badenian) exhumation of the SzD with the formation of a series of high-angle normal faults and the deposition of Pannonian clastic sediments. **d)** Recent hydraulic system of the SzD following Late Miocene subsidence of the area with significant overpressure under the local aquitard (Endrőd Formation) and the evolution of the "chimney structure". The cross sections are not to scale.

the crystalline rock body (VASS et al., 2009). The evaluation of the diagenetic history (JUHÁSZ et al., 2002) also demonstrated that the basement rocks and the overlying sediments must have been hydraulically connected since the Middle Miocene. This evidence underlines the importance of the intensely fractured parts of the AG group and the damage zones of the major fault zones in both the palaeo- (based on fluid inclusion data) and recent (based on production data and modeling) hydrogeological systems of the SzD despite the differences that were caused by the complex Neogene evolution of the SzD (JUHÁSZ et al., 2002; M. TÓTH, 2008).

7. CONCLUSIONS

(1) In this study, we identified the master fault zones of the Szeghalom Dome, which is one of the largest fractured basement hydrocarbon reservoirs in the Pannonian Basin. According to previous investigations, these wide fault zones are mainly related to post-metamorphic tectonic events and possibly act as migration pathways because of their higher porosity and permeability.

(2) Based on integrated evaluations of core and well-log data, 1D lithostratigraphic columns of wells were defined and correlated spatially. The tectonized intervals were distinguished from the undeformed wallrock, and their internal lithological structures (fault breccias, cataclasites, fault gouges) were defined to determine the significant components of these zones (damage zone versus fault core). We characterized the master faults as intervals consisting of extensive fault gouge zones.

(3) The spatial arrangement of the fault zones indicates the presence of low angle thrust faults; based on the evolution of the Pannonian Basin, these faults were interpreted as indications of Cretaceous nappe activity. The structure of the Szeghalom Dome was further complicated by middle Miocene extension, which formed blocks in a horst-graben geometry and culminated in the exhumation of the metamorphic high.

(4) The data on the structural evolution of the Szeghalom basement high were integrated with the results of previous investigations on the fracture network geometry, palaeo-fluid evolution and recent production data. The results suggest that the amphibolite bodies have the highest storage capacity in the basement reservoir; the amphibolites are located exclusively within the AG lithologic group in the structurally highest basement locations.

(5) The strong chemical dissimilarities of the hydrocarbon-bearing fluid inclusions that are trapped in fracture-filling quartz veins can be explained by several theories but probably developed due to the significant permeability anisotropy in the fault zones that was derived from their complex architecture coupled with the effect of the Neogene structural evolution on the local flow systems.

(6) A comparison of the palaeo- and recent petroleum systems of the Szeghalom Dome revealed that the main difference was caused by the different source rocks of the hydrocarbons. The fault zones played a key role in the migration of the hydrocarbons from adjacent overpressured sub-basins to both the amphibolite bodies and, since at least the middle Miocene, to the overlying clastic sediments.

ACKNOWLEDGEMENT

We thank MOL Hungarian Oil and Gas Company for providing the samples, datasets and the financial support of this research. Balázs KISS (MOL) is thanked for the fruitful discussions about the behaviour of the Szeghalom reservoir. Reviews by István BÉRCZI and Gyula MAROS have significantly improved the manuscript, and are much appreciated. English was corrected by American Journal Experts.

REFERENCES

ALBU, I. & PÁPA, A. (1992): Application of high-resolution seismics in studying reservoir characteristics of hydrocarbon deposits in Hungary.– Geophysics, 57, 1068–1088.

ALLAN, U.S. (1989): Model for hydrocarbon migration and entrapment within faulted structures.– AAPG Bulletin, 73, 803–811.

BEN-ZION, Y. & SAMMIS, C.G. (2003): Characterization of fault zones: Pure and Applied Geophysics, 160, 677–715.

CAINE, J.S., EVANS, J.P. & FORSTER, C.B. (1996): Fault zone architecture and permeability structure.– Geology, 24, 1025–1028.

CSONTOS, L. & NAGYMAROSY, A. (1998): The Mid-Hungarian line: a zone of repeated tectonic inversions.– Tectonophysics, 297, 51–71.

EVANS, J.P., FORSTER, C.B. & GODDARD, J.V. (1997): Permeability of fault-related rocks and implications for fault-zone hydraulic structure.– Journal of Structural Geology, 19, 1393–1404.

GÉRAUD, Y., DIRAISON, M. & ORELLANA, N. (2006): Fault zone geometry of a mature active normal fault: A potential high permeability channel (Pirgaki fault, Corinth rift, Greece).– Tectonophysics, 426, 61–76.

HORVÁTH, F., DÖVÉNYI, P., SZALAY, Á. & ROYDEN, L.H. (1988): Subsidence, thermal and maturation history of the Great Hungarian Plain.– In: ROYDEN, L.H. & HORVÁTH, F. (eds.): The Pannonian Basin: A Study in Basin Evolution.– AAPG Memoir, 43, 355–372.

HORVÁTH F., BADA G., SZAFIÁN P., TARI G., ÁDÁM, A. & CLOETINGH, S.(2006): Formation and deformation of the Pannonian basin: constraints from observational data.– In: GEE, D.G. & STEPHENSON, R.A. (eds.): European Lithosphere Dynamics, Geological Society, London.– Memoirs, 32, 191–206.

HUNG, J., WU, Y., YEH, E. & WU, J. (2007): Subsurface Structure, Physical Properties, and Fault Zone Characteristics in the Scientific Drill Holes of Taiwan Chelungpu-Fault Drilling Project– Terrestrial Atmospheric Oceanic Science, 18, 271–293.

JEPPSON, T.N., BRADBURY, K.K. & EVANS, J.P. (2010): Geophysical properties within the San Andreas Fault Zone at the San Andreas Fault Observatory at Depth and their relationships to rock properties and fault zone structure.– Journal of Geophysical Research, 115, B12423.

JUHÁSZ, A., M TÓTH, T., RAMSEYER, K. & MATTER, A. (2002): Connected fluid evolution in fractured crystalline basement and overlying sediments, Pannonian Basin, SE Hungary.– Chemical Geology, 182, 91–120.

KOVÁCS, S., SZEDERKÉNYI, T., HAAS, J., BUDA, GY., CSÁSZÁR, G. & NAGYMAROSY, A. (2000): Tectonostratigraphic terranes in the pre-Neogene basement of the Hungarian part of the Pannonian area.– Acta Geologica Hungarica, 43, 225–328.

LŐRINCZ, K.D. (1996): Determination of stress-field history on the basis of multiphase tectonism identified in the seismic profiles, in the Western part of the Szolnok flysch belt.– Magyar Geofizika, 37, 228–246 (in Hungarian with English abstract).

M. TÓTH, T., HOLLÓS, CS., SZŰCS, É. & SCHUBERT, F. (2004): Conceptual fracture network model of the crystalline basement of the Szeghalom Dome (Pannonian Basin, SE Hungary).– Acta Geologica Hungarica, 47, 19–34.

M. TÓTH, T. (2008): Repedezett, metamorf fluidumtárolók az Alföld aljzatában.– Academic Doctoral Thesis (In Hungarian).

M. TÓTH, T., REDLERNÉ TÁTRAI, M. & KUMMER, I. (2009): Structural evolution of the Szeghalom metamorphic dome on the basis of petrological and seismic data Magyar.– Geofizika, 43, 143–151. (In Hungarian with English abstract).

MANZOCCHI, T., CHILDS, C. & WALSH, J.J. (2010): Faults and fault properties in hydrocarbon flow models.– Geofluids, 10, 94–113.

MÁTYÁS, J. (1994): Diagenesis and porosity evolution of Neogene reservoir sandstones in the Pannonian Basin (southeast Hungary), PhD thesis, University of Bern, 196 p.

MOELLER-PEDERSEN, P. & KOESTLER, A.G. (1997): Hydrocarbon Seals Importance for Exploration and Production, Norwegian Petroleum Society, Special Publications No. 7., Elsevier Science, Singapore, 250 p.

MOLNÁR, L., M. TÓTH, M. & SCHUBERT, F. (2014): Statistical characterization of brittle and semi-brittle fault rocks: a clast geometry approach.– Acta Geodaetica et Geophysica, (In Press) doi number: 10.1007/s40438-014-0067-3

MORT, K. & WOODCOCK, N.H. (2008): Quantifying fault breccia geometry: Dent Fault, NW England.– Journal of Structural Geology, 30, 701–709.

NELSON, R.A., 2001. Geologic Analysis of Naturally Fractured Reservoirs. 2nd Edition, Gulf Publishing Company Book Division, Houston, 322 p.

PAP, S. (1990): Thrust-faulted sequences in Transtisia.– Special Publications of the Hungarian Geological Survey, Budapest (In Hungarian with English abstract).

POSGAY, K., BODOKY, T., HEGEDŰS, E., KOVÁCSVÖLGYI, S., LENKEY, L., SZAFIÁN, P., TAKÁCS,E., TIMÁR, Z. & VARGA,G. (1995): Asthenospheric structure beneath a Neogene basin in southeast Hungary.– In: CLOETINGH, S., D'ARGENIO, B., CATALANO, R., HORVÁTH, F. & SASSI, W. (eds): Interplay of extension and compression in basin formation.– Tectonophysics, 252, 467–484.

SCHUBERT, F. (2003): Reconstruction of hydrocarbon-bearing fluid migration in the Szeghalom Dome (SE Hungary).– PhD thesis, University of Szeged, 158 p. (in Hungarian).

SCHUBERT, F., DIAMOND, L.W. & M. TÓTH, T. (2007): Fluid-inclusion evidence of petroleum migration through a buried metamorphic dome in the Pannonian Basin, Hungary.– Chemical Geology, 244, 357–381.

STORTI, F., BALSAMO, F. & SALVINI, F. (2007): Particle shape evolution in natural carbonate granular wear material.– Terra Nova, 19, 344–352.

SZEDERKÉNYI, T., ÁRKAI, P. & LELKES-FELVÁRI, GY. (1991): Crystalline groundfloor of the Great Hungarian Plain and South Transdanubia.– In: KARAMATA, S. (ed.): Geodynamic evolution of the Pannonian Basin, Beograd, 261–273.

TARI, G., HORVÁTH, F. & RUMPLER, J. (1992): Styles of extension in the Pannonian Basin.– Tectonophysics, 208, 203–219.

TARI, G., DÖVÉNYI, P., DUNKL, I., HORVÁTH, F., LENKEY, L., STEFANESCU, M., SZAFIÁN, P. & TÓTH, T. (1999): Lithospheric structure of the Pannonian basin derived from seismic, gravity and geothermal data.– In: DURAND, B., JOLIVET, L., HORVÁTH, F. & SÉRANNE, M. (eds.): The Mediterranean Basins: Tertiary Extension within the Alpine Orogen. Geological Society, London, Special Publications, 156, 215–250.

TELEKI, P.G., MATTICK, R.E. & KÓKAI, J. (eds.) (1994): Basin Analysis in Petroleum Exploration. A Case Study from the Békés Basin, Hungary. Kluwer Academic Publishers.

VASS, I., M. TÓTH, T., SZANYI, J. & KOVÁCS, B. (2009): Water and heat flow through uplifted metamorphic highs in the basement of the Pannonian Basin.– In: M. TÓTH, T. (ed.): Igneous and metamorphic rocks of the Tisza Unit. Szeged, Geolitera press, 325–339 p. (In Hungarian with English abstract).

WIBBERLEY, C.A.J. & SHIMAMOTO, T. (2003): Internal structure and permeability of major strike-slip fault zones: the Median Tectonic Line in Mie Prefecture, Southwest Japan.– Journal of Structural Geology, 25, 59–78.

ZHANG, S., TULLIS, T. & SCRUGGS, V. (2001): Implication of permeability and its anisotropy in a mica gouge for pore pressure in fault zones.– Tectonophysics, 335, 37–50.

Manuscript received September 11, 2014
Revised manuscript accepted July 05, 2015
Available online October 31, 2015